Numerical modelling of the compaction behaviour of crushed rock salt

U.Heemann & S.Heusermann
Federal Institute for Geosciences and Natural Resources (BGR), Hannover, Germany

W.Sarfeld
Sarfeld Research and Development (SRD), Berlin, Germany

B.Faust
Ingenieurbüro Faust & Fritsche (IFF), Berlin, Germany

ABSTRACT: The disposal of heat-generating radioactive waste includes the options of emplacement of casks in drifts of a repository in salt rock, and the emplacement of canisters in boreholes. The use of crushed salt as backfill material is planned to seal drifts and boreholes. The prediction of the long-term behaviour of backfilled drifts and boreholes requires the development of appropriate numerical models. To this end, a new constitutive model for crushed salt based on phenomenological and physical assumptions was developed and implemented into the ANSALT finite element code, including the necessary numerical algorithms for efficient evaluation of the nonlinear time-dependent behaviour of crushed salt. To demonstrate the suitability of the code and the constitutive model, calculations on a large-scale in-situ test of the emplacement of heated casks in drifts are presented which focus on the long-term thermomechanical behaviour of backfilled drifts, e.g. drift closure, backfill pressure, and backfill compaction.

1 INTRODUCTION

The German concept for the disposal of heat-generating radioactive waste in a repository in salt rock involves two methods: (1) The drift emplacement concept was developed for the direct disposal of spent fuel rods in casks which are emplaced on the floor of drifts. (2) In the borehole emplacement concept, high level waste canisters are deposited in vertical boreholes drilled several hundred meters beneath repository drifts. Backfilling is required to seal these drifts and boreholes after waste emplacement. The function of the backfill is to act as a geotechnical long-term barrier against inflowing brine or water, to conduct the heat generated by radioactive decay from the waste to the host rock, and to stabilize the process of drift and borehole closure.

Crushed salt was selected as the most suitable backfill material. As a consequence of the time-dependent closure of drifts and boreholes caused by thermomechanical creep of the salt rock, the crushed salt will be compacted and its initial porosity and permeability will decrease. Over long time periods, the crushed salt is expected to gradually reconsolidate into a material comparable to virgin rock salt.

The understanding of the thermomechanical compaction behaviour of crushed salt is an important precondition for repository design and for long-term safety assessment. The use of appropriate numerical models is necessary to predict the behaviour of backfilled drifts and boreholes. To this end, a constitutive model for crushed salt was developed and was implemented into the ANSALT finite element code, including the necessary numerical algorithms for efficient calculations, focussing in particular on the nonlinear time-dependent behaviour of crushed salt and salt rock.

2 MATERIAL MODEL FOR CRUSHED SALT

The model used here is an enhanced version of the model of Zhang et al. (1995) based on phenomenological and physical assumptions. This originally purely hydrostatic model is of Norton type similar to the description of deviatoric creep of rock salt (Equation 1)

$$\dot{\underline{\varepsilon}}_{d,\,rock\ salt} = A\ \exp\left(\frac{-Q}{R\ T}\right) q^{n}\ \frac{3}{2}\ \frac{\underline{S}}{q} \qquad (1)$$

while for crushed salt Zhang found (Equation 2)

$$\dot{\underline{\varepsilon}}_{v,\,crushed\ salt\_Zhang} = A_v\ \exp\left(-\frac{Q}{RT}\right)\left(\frac{p}{U}\right)^{n_v}\ \underline{1}\ , \qquad (2)$$

$$U = \ln\left(\frac{e_o}{e}\right)^{d_v} = \ln\left(\frac{\varepsilon_{v_E}}{\varepsilon_{v_E} - \varepsilon_v}\right)^{d_v} . \qquad (3)$$

$\dot{\underline{\varepsilon}}_d$ and $\dot{\underline{\varepsilon}}_v$ represent creep (deviatoric) and compaction rate (volumetric), temperature behaviour is

described for both of them by an exponential function (Arrhenius-term) of activation energy Q, gas constant R and temperature T. While for pure rock salt creep, stress dependency is simply given by a power of equivalent stress q (for quasi stationary creep), in the case of crushed salt, the compaction rate depends on a power of hydrostatic stress p over a geometrical function U. This function U has been determined by phenomenological deduction from experimental data, and it can be interpreted as very similar to a relative contact area, giving the active stress p_{act} = p/U in the creep zone. For the initial state (e = e_o) in the case of hydrostatic stress, the compaction rate is infinite, but tends to zero for zero void ratio.

A modification of this simple model was necessary for several reasons.

- In real situations the model also has to take into consideration deviatoric stress and strain rate.
- For high compaction it should match the behaviour of rock salt.
- Oedometric tests (Stührenberg & Zhang, 1995) seemed to prove that crushed salt has a stress power much higher than that of rock salt, and even increases with higher porosity.

In the case of deviatoric loading, the physical phenomena at the level of grains and their contact areas are very similar to that of hydrostatic loading. Due to the irregular distribution of grains, in both cases compaction, gliding and rolling occur to a similar degree. For the new approach, the deviatoric creep element was thus constructed by replacing the compaction rate tensor by a deviatoric creep rate tensor $\underline{\dot{\varepsilon}}_d$ and hydrostatic stress p by its deviatoric counterpart q in a first attempt (see Equation 4). The function was extended by an exponential stress term to incorporate the change of stress exponent already mentioned. To achieve a pure power law dependency for zero porosity, the geometric function U within the power term had to be replaced by a slightly modified function U_1 tending to 1 instead of infinity for zero void ratio. U_1 is defined below. Thus, most parameters (A, Q and n) are already fixed by the behaviour of rock salt (see Equation 1).

$$\underline{\dot{\varepsilon}}_d = A \ \exp\left(\frac{-Q}{R\ T}\right)\left(\frac{q}{U_1}\right)^n \ \exp\left(\frac{\gamma\ q}{U}\right)\frac{3}{2}\frac{\underline{S}}{q} \qquad (4)$$

As mentioned above, deviatoric creep and compaction require a very similar description. Equation 5 describing compaction rate in the modified model differs from Equation 4 in its first part mainly by hydrostatic stress and the supplemented denominator α. In Equation 5, the unit tensor instead of the deviatoric tensor construction is obligatory.

$$\underline{\dot{\varepsilon}}_v = A\exp\left(\frac{-Q}{RT}\right)\left(\frac{p}{\alpha U_1}\right)^n \exp\left(\frac{\gamma\, p}{\alpha U}\right)\frac{e}{e_o(1+e)}\underline{1} \qquad (5)$$

α, effectively being a function (see below), is necessary due to the arbitrariness in the definition of deviatoric and hydrostatic stresses. For instance, the 2nd invariant in one case and the trace of stress tensor in the other case could also have been chosen. But at least for high porosity, α should be of the order of 1.

High porosity compaction as well as creep are mainly determined by the creep of salt at the contact zone. This has been taken into account by the function U. However, in the case of very low porosity, the mechanism principally changes, and compaction rate should be more or less proportional to the void ratio - similar to closure of caverns or drifts in salt rock. That means:

$$\dot{V} = k\ \ V\ \ (A\ \ \sigma_{rock}^{n}) \qquad (6)$$

in caverns etc. and analogously for void ratios:

$$\dot{e} \propto e\,. \qquad (7)$$

The term in brackets in Equation 6 is an abbreviated form of the Norton law (see Equation 1), but taken here as a function of the (hydrostatic) rock pressure. The factor k depends on the geometry of the cavern. Taking account of the relation

$$\dot{\varepsilon}_v = \frac{\dot{e}}{1+e} \qquad (8)$$

the above outlined considerations can be combined, and result in Equation 5. For low compaction, where e is close to e_o, the last two fractions of Equation 5 give a result slightly less than 1 changing very smoothly compared to the influence of functions U and U_1. For high compaction (and constant stress), the Norton term does not change further, nor does the exponential function for which the argument is approaching zero. This therefore results in a behaviour similar to that of Equation 6 or 7. The value of α has to change for low porosity to take into consideration factor k.

The functions U, U_1 and α are listed below. The parameter e_c denotes the transition void ratio where creep dominated by the contact zones changes to creep dominated by the closure of voids (small caverns).

$$U = \left(\ln\left(\frac{e_o}{e}\right)\right)^d, \quad U_1 = \left(\frac{\ln\left(\frac{e_o+e_c}{e+e_c}\right)}{\ln\left(\frac{e_o+e_c}{e_c}\right)}\right)^d, \qquad (9, 10)$$

$$\alpha = \alpha_o + \beta\ \exp\left(-\frac{e}{e_c}\right) \qquad (11)$$

The parameter values already known for rock salt were used and only the remaining parameters had to

be fitted to the data. Comparison with data on triaxially loaded crushed salt (Korthaus, 1996) showed that the exponential term in Equation 5 can be neglected for crushed salt. The parameter γ thus was set to zero. The parameter values have been tabulated in Table 1.

Table 1: Parameter values for the above described model, defined by Equations 4, 5, 9, 10 and 11.

A	0.18 d^{-1} MPa^{-n}	e_c	0.077
Q	54.0 kJ/(mole K)	γ	0
n	5	α_o	1.341
d	1.402	β	1.187

Theoretical work of Heemann (1993) as well as experimental work of Walter (1995) on the elastic behaviour of crushed salt led to a more or less linear relation between compaction and elastic modulus such that it reaches the value of rock salt for full compaction while Poisson's ratio remains constant.

$$E_{crushed\ salt} = \frac{e}{e_o}\ E_{rock\ salt}\ , \qquad \nu = \text{const} \qquad (12, 13)$$

3 NUMERICAL ALGORITHMS

An objective of this paper is to present an effective procedure based on finite element analysis for creep problems with temperature-dependent material properties. The basis of the algorithm for the analysis of the largely nonlinear creep problem is the α-method. The resulting nonlinear algebraic equations are solved by a modified NEWTON-RAPHSON iteration scheme. The following expression for the multiaxial creep strain rate is used

$$\dot{\varepsilon}^c_{ij} = \frac{1}{3}\dot{\varepsilon}^h \delta_{ij} + \frac{3}{2}\frac{1}{q}\dot{\varepsilon}^d \sigma^d_{ij}\ . \qquad (14)$$

3.1 *Constitutive equation*

For the constitutive equation, it is assumed that the elastic and incremental creep strains are additive

$$\Delta\varepsilon_{ij} = \Delta\varepsilon^e_{ij} + \Delta\varepsilon^c_{ij} \qquad (15)$$

$$\Delta\sigma_{ij} = C^e_{ijkl}\,(\Delta\varepsilon_{kl} - \Delta\varepsilon^c_{kl}) = C^e_{ijkl}\,\Delta\varepsilon^e_{kl} \qquad (16)$$

where C^e_{ijkl} is the elastic constitutive tensor. Inverting Equation 16 leads to the following expression for the incremental elastic strains (Anderson, 1976)

$$\Delta\varepsilon^e_{ij} = C^{e\ -1}_{ijkl}\Delta\sigma_{kl}\ . \qquad (17)$$

3.2 *Creep strains*

In order to compute the incremental creep strains, the following α-algorithm is used

$$\Delta\varepsilon^c_{ij} = \int_t^{t+\Delta t} \dot{\varepsilon}^c_{ij}\,d\tau = {}^{t+\alpha\Delta t}\dot{\varepsilon}^c_{ij}\,\Delta t = {}^t\dot{\varepsilon}^c_{ij} + \alpha\Delta\dot{\varepsilon}^c_{ij}\ . \qquad (18)$$

Expanding $\Delta\dot{\varepsilon}^c_{ij}$ into a Taylor series and ignoring the derivations due to the void ratio and temperature, the total differential for the incremental creep strain rate can be expressed as

$$\Delta\dot{\varepsilon}^c_{ij} = \left[\frac{3}{2}\frac{\varepsilon^d}{q}\left[\delta_{ik}\delta_{jl} - \frac{1}{3}\delta_{ij}\delta_{kl} + \frac{2}{3}\frac{1}{q}\left(\frac{n-1}{q} + \frac{\gamma}{U}\right)\sigma^d_{ij}\sigma^d_{kl}\right] + \frac{1}{3}\varepsilon^v\left[\frac{1}{3}\left(\frac{n}{p} - \frac{\gamma}{\alpha^c U}\right)\delta_{ij}\delta_{kl}\right]\right]\Delta\sigma_{kl}\ . \qquad (19)$$

In short form Equation 19 can be written as

$$\Delta\dot{\varepsilon}^c_{ij} = D^c_{ijkl}\,\Delta\sigma_{kl}\ . \qquad (20)$$

Substituting Equation 20 in Equation 18 the creep strains denote as

$$\Delta\varepsilon^c_{ij} = {}^t\dot{\varepsilon}^c_{ij} + \alpha\, D^c_{ijkl}\,\Delta\sigma_{kl}\ \Delta t\ . \qquad (21)$$

3.3 *Stresses*

Using Equation 17 and Equation 21, an expression for the stress tensor is obtained

$$\Delta\sigma_{ij} = \left[C^{e\ -1}_{ijkl} + \alpha\, D^c_{ijkl}\Delta t\right]^{-1}\left[\Delta\varepsilon_{kl} - {}^t\dot{\varepsilon}^c_{ij}\,\Delta t\right]. \qquad (22)$$

Introducing the stress $\boldsymbol{s}$, total strain $\boldsymbol{e}$ and the creep strain $\boldsymbol{e}^c$, Equation 22 denotes in vector form

$$\Delta\mathbf{s} = \left[\mathbf{C}^{-1} + \alpha\mathbf{D}^c\,\Delta t\right]^{-1}\left[\Delta\mathbf{e} - \Delta\,{}^t\mathbf{e}^c\,\Delta t\right]. \qquad (23)$$

3.4 *Finite element formulation*

The finite element method is used to analyze the compaction of crushed salt. The basic equation written in an incremental form is given by

$$\int_V \delta\Delta\mathbf{e}^T\Delta\mathbf{s}\,dV - \delta\mathbf{u}\,\Delta\mathbf{f} = 0 \qquad (24)$$

where $\Delta\mathbf{f}$ is the load vector and $\delta\mathbf{u}$ the displacement vector.

Using the strain-displacement matrix, the total strains can be expressed as functions of the displacement vector $\mathbf{e} = \mathbf{B}\,\mathbf{u}$. Substituting this relation and Equation 23 into Equation 24 yields the following expression for the equilibrium

$$\delta \mathbf{u}^T \mathbf{K}^{ec} \Delta \mathbf{u} = \delta \mathbf{u}^T \left[\Delta \mathbf{f}^c + \Delta \mathbf{f} \right] \tag{25}$$

where $\mathbf{K}^{ec}$ is the tangential stiffness matrix, $\Delta \mathbf{f}$ the load vector and $\Delta \mathbf{f}^c$ the load vector resulting from the creep strains

$$\mathbf{K}^{ec} = \int_V \mathbf{B}^T \left[\mathbf{C}^{-1} + \alpha \mathbf{D}^c \, \Delta t \right]^{-1} \mathbf{B} \, dV \tag{26}$$

$$\Delta \mathbf{f}^c = \int_V \mathbf{B}^T \, {}^t\dot{\mathbf{e}}^c \Delta t \, dV \ . \tag{27}$$

3.5 *Iteration of material law*

The stresses have to be integrated during the computation of the equilibrium to achieve an accurate solution and an efficient analysis of the time-dependent behaviour of crushed salt and rock salt. Since the stresses are computed with an implicit integration method (Snyder & Bathe, 1981), iteration is required while integrating the stresses, in addition to the iteration of equilibrium

$$\Delta \mathbf{s} = \int_{{}^t\mathbf{e}}^{{}^{t+\Delta t}\mathbf{e}} \mathbf{C}^{\mathbf{e}} \, d(\mathbf{e} - \mathbf{e}^{\mathbf{c}}) \ . \tag{28}$$

In order to compute the stresses, Equation 28 is divided into subincrements and a successive iteration scheme is developed

$$\mathbf{e}^c_{k+1} = {}^{t+\alpha\Delta t}\dot{\mathbf{e}}^c_k ({}^{t+\alpha\Delta t}\mathbf{s}_k) \, \Delta t \tag{29}$$

$$\Delta \mathbf{s}_{k+1} = {}^{t+\alpha\Delta t}\mathbf{C}^e \left[\Delta \mathbf{e} - \Delta \mathbf{e}^c_{\mathbf{k+1}} \right] \ . \tag{30}$$

This scheme above shows a slow rate of convergence. In order to improve this rate, the equations above are solved using the NEWTON-RAPHSON iteration. The incremental creep strain was expanded into a two-term TAYLOR series about the k^{th} approximate solution

$${}^{t+\alpha\Delta t}\mathbf{e}^c_{k+1} = {}^{t+\alpha\Delta t}\mathbf{e}^c_k + \left[\frac{\partial \, {}^{t+\alpha\Delta t}\Delta \mathbf{e}^c}{\partial \, {}^{t+\alpha\Delta t}\Delta \mathbf{s}} \right]_k \left[\Delta \mathbf{s}_{k+1} - \Delta \mathbf{s}_k \right] \ . \tag{31}$$

Substituting Equation 31 into Equation 30 leads to an expression for the stresses

$$\begin{aligned} \Delta \mathbf{s}_{k+1} = & \left[\mathbf{I} + \alpha \Delta t \, {}^{t+\Delta t}\mathbf{C}^e \left[\frac{\partial \, {}^{t+\alpha\Delta t}\Delta \mathbf{e}^c}{\partial \, {}^{t+\alpha\Delta t}\Delta \mathbf{s}} \right]_k \right]^{-1} \\ & \left[{}^{t+\Delta t}\mathbf{C}^e \left[\Delta \mathbf{e} - \Delta \mathbf{e}^c_k \right] + \right. \\ & \left. \alpha \Delta t \, {}^{t+\Delta t}\mathbf{C}^e \left[\frac{\partial \, {}^{t+\alpha\Delta t}\Delta \mathbf{e}^c}{\partial \, {}^{t+\alpha\Delta t}\Delta \mathbf{s}} \right]_k \right] \Delta \mathbf{s}_k \end{aligned} \tag{32}$$

3.6 *Results*

The material model and solution procedure in chapters 3.2 and 3.3 have been implemented in the ANSALT finite element computer program. Several tests on accuracy, stability, and geometric nonlinear capability were carried out on the algorithms (e.g. a rotating specimen under compression or a rod being bent into a ring). The simulation of a uniaxial compression test is presented here as an example.

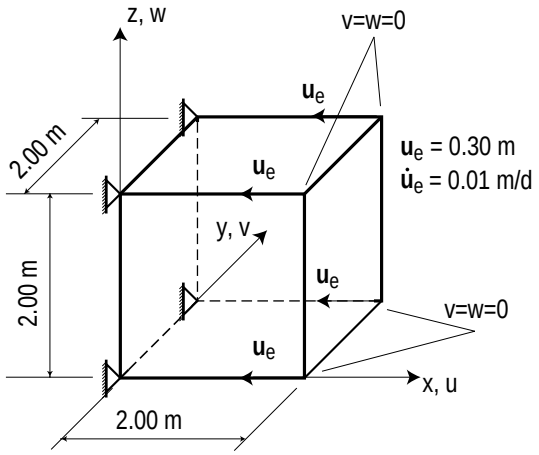

Figure 1. Numerical model (uniaxial compression test).

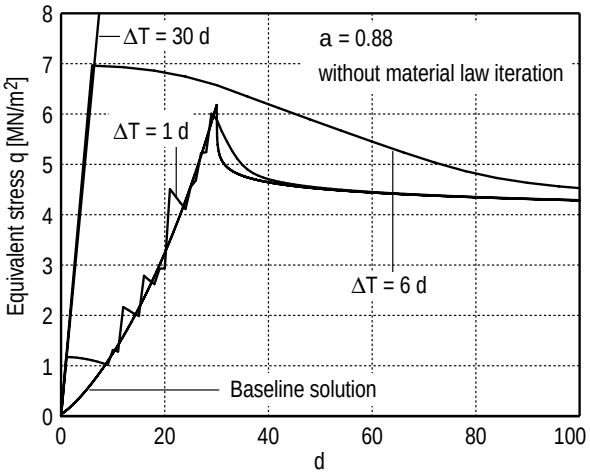

Figure 2. Equivalent stress without iteration of the material law

A rectangular specimen with a length of l = 2 m is subjected to a displacement of $u_{\max}$ = 0.3 m within 30 days in horizontal direction, the displacement rate being constant with $\dot{u} = 0.01\,\text{m/d}$. The reverse of the specimen and the displacements in the transverse and vertical direction are fixed (Figure 1).

Figures 2 and 3 show the transient distribution of the equivalent and hydrostatic stresses. The time steps vary from $\Delta t = 0.01$ d to $\Delta t = 30$ d. Without consideration of the material law iteration, the solutions become increasingly unstable for time steps bigger than $\Delta t = 1.0\,\text{d}$, on the other hand, the solutions remain stable when material law iteration is included.

In order to guarantee a stable and exact solution for nonlinear creep problems, an implicit integration of the stresses has to be carried out in addition to the iteration of the equilibrium.

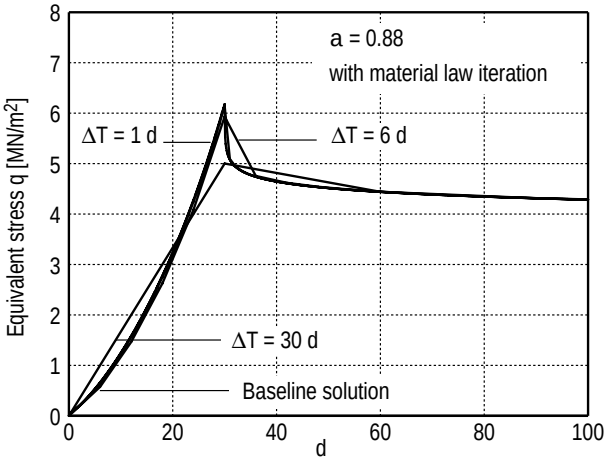

Figure 3. Equivalent stresses with iteration of the material law

4 MODELLING OF THE TSDE TEST

4.1 *Model description*

The above described constitutive model was used within the "Comparative Study on Crushed Salt (CS^2)" benchmark project (Heemann et al., 1999) – among others – to calculate the geomechanical situation within the TSDE test, a large-scale in-situ test on the "Thermal Simulation of Drift Emplacement" in the Asse mine (Lower Saxony, Germany). The test drifts are 800 m below ground, backfilled with crushed salt and heated by emplaced heater casks simulating the heat production of radioactive waste. A plot of the two-dimensional model is shown in Figure 4.

Three heaters, each 5.5 m long, are placed in two parallel drifts, one behind the other and with a distance of 3 m. Therefore, axisymmetric conditions can be assumed. The host material is pure rock salt. Excavation of the drifts, emplacement of the heaters, backfilling with crushed salt and the start of heating are assumed to take place instantaneously. The initial stress was set to 12 MPa without accounting for gravity. The model run time was set to 10 years.

The test field comprises a large number of sensors and gauges measuring various parameters, e.g. temperature, deformation and stress. Thus, comparison with experimental data was done along a vertical and a horizontal line through the drift.

The thermal properties of the crushed salt change with compaction. Due to the fact that ANSALT is not capable of full thermomechanical coupling, the complete calculation had to be carried out iteratively by a thermal calculation with the separate code ANTEMP followed by the mechanical calculation over about the same time. The change of void ratio then resulted in new thermal properties used as input for a new calculation cycle. For this purpose, the crushed salt was divided into 4 "rings" around the heater with different levels of compaction, with the aim of

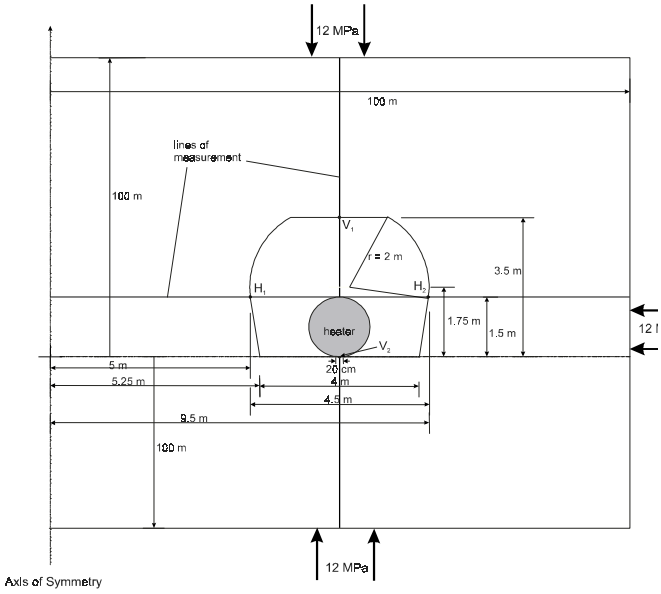

Figure 4. Sketch of the two-dimensional model of the backfilled and heated drift. The left border represents a line of symmetry.

taking into account the inhomogeneous thermal conductivity. In fact, near the corner between the heater and the floor there was some deviation from the arbitrary classification. But in practice, no relevant influence on the main results is expected.

4.2 *Numerical results*

Temperature calculations showed very good agreement with the experimental data for 1 year after the start of heating. After 3 years, distinct differences appeared, and after 10 years, agreement was poor. This is associated with the two-dimensional modelling which is only adequate for short periods of time (perhaps 1 or 2 years). But when the radial expansion of the temperature field tends to half of the axial length of the test field (orthogonal to the model plane), three-dimensional effects gain in importance. Axial heat conduction effectively leads to strong cooling compared to the model, thus keeping the temperature considerably lower than in case of the model.

There is no doubt from former calculations that heating has an important influence on the closure of drifts, not only because of its effect on creep rate but even more due to the thermal expansion of the rock salt. Thus, closure of the drift is strongly enhanced in the model by the higher temperature (s. Figure 5).

Because of the high rates of drift closure, the model gave very high compactions for the crushed salt. Whilst it was found that void ratio in situ is of the order of 31 % after eight years, crushed salt in the model is very near to full compaction after 10 years (s. Figure 6, the values for the innermost ele-

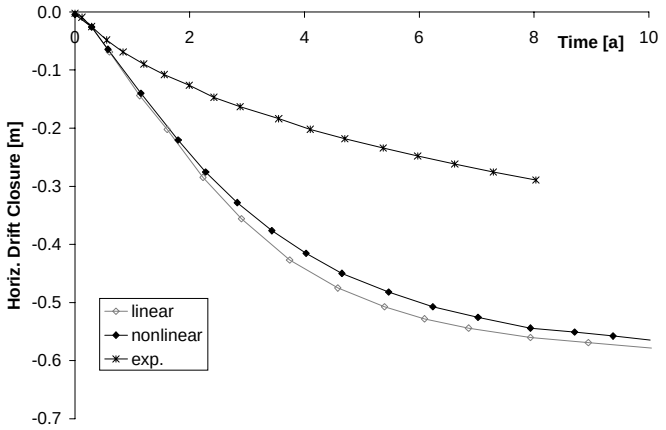

Figure 5. Calculated closure of the drift compared to experimental data.

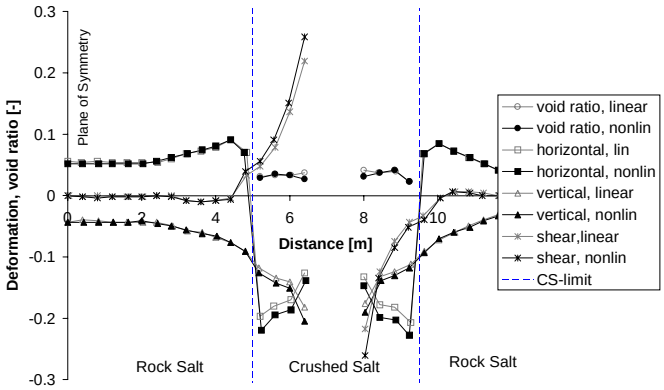

Figure 6. Deformation within crushed salt and proximal rock salt. Void ratio is also displayed.

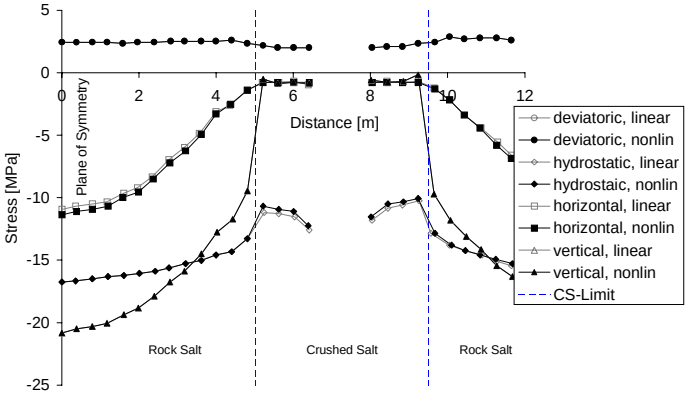

Figure 7. Stresses in the crushed salt and the proximal rock salt.

ments have been omitted due to an interpolation with the neighbouring heater done by the postprocessor). The stresses within the crushed salt and the host rock are displayed in Figure 7.

4.3 *Numerical behaviour*

After having found an appropriate value for the α-value in the integration method, the calculations were essentially very stable and fast. Starting with steps of 1 day model time, these were increased to 50 d at 10 years, resulting in a total of 221 steps. With typically 7 iterations, this needed about 127 min cpu-time on an HP V-class/2200. It was shown that even with half the number of steps and only few more iterations, a stable calculation was possible without significant differences.

5 SUMMARY AND CONCLUSIONS

A new constitutive model has been developed to describe the thermomechanical behaviour of crushed salt. The model includes both hydrostatic and deviatoric compaction behaviour.

Numerical algorithms required for an efficient solution procedure based on the finite element method are presented. Both the constitutive model and the numerical algorithms were implemented into the ANSALT finite element code. Accuracy, stability, and geometrical nonlinear capability were tested by simulation of a simple uniaxial compression test.

Thermomechanical calculations were carried out on a large-scale in-situ test involving the emplacement of heated casks in backfilled drifts to compare the numerical results to experimental test data.

The results showed that the constitutive model for crushed salt and the numerical algorithms developed for use in the ANSALT code provide an efficient, stable and accurate method to predict the thermomechanical behaviour of excavations in salt rock backfilled with crushed salt.

REFERENCES

Anderson, C.A. 1976. An investigation of the steady creep of a spherical cavity in a half space. *Journal of Applied Mechanics*, Vol. 98, No. 2, pp.254-258.

Heemann, U., S. Heusermann & N.C. Knowles 1999. Benchmarking the behaviour of crushed salt - the CEC BAMBUS project. *7th Int. Conf. NAFEMS*, Rhode Island, USA, 25-28 April.

Heemann, U. 1993. Theoretical calculation of the elastic properties of crushed salt. Unpublished.

Korthaus, E. 1996. Consolidation and deviatoric deformation behaviour of dry crushed salt at temperatures up to 150°C. *4th Conference on the Mechanical Behaviour of Salt*, Montreal.

Snyder, D. & K.J. Bathe 1981. A solution procedure for thermo-elastic-plastic and creep problems. *Nuclear Engineering and Design*, Vol. 64, pp.49-80, 1981.

Stührenberg, D. & C.L. Zhang, 1995. Untersuchungen zum Kompaktionsverhalten von Salzgrus als Versatzmaterial für Endlagerbergwerke im Salz unter besonderer Berücksichtigung der Wechselwirkung zwischen Gebirge und Versatz. *BGR-Bericht*, Archiv-Nr. 113 259, Hannover.

Walter, F. 1995. Internal report of GSF, Braunschweig.

Zhang, C.L., U. Heemann, M.W. Schmidt, G. Staupendahl 1995. Constitutive model for the description of compaction behaviour of crushed salt backfill. *Proc. ISRM Int. Symp. EUROCK'95*.